Multireference Singles and Doubles Configuration Interaction Study of the Electronic States of GaSb

Antara Dutta, Anjan Chattopadhyay, and Kalyan Kumar Das*

Physical Chemistry Section, Department of Chemistry, Jadavpur University, Calcutta 700 032, India

Received: June 2, 2000; In Final Form: August 4, 2000

Spectroscopic properties of low-lying electronic states of gallium antimonide (GaSb) have been studied by using ab initio based large scale multireference singles and doubles configuration interaction (MRDCI) calculations. Relativistic effective core potentials (RECP) of Ga and Sb are employed in the calculations. Potential energy curves of all 34 Λ−S states which correlate with the three lowest dissociation limits, namely, $Ga(^2P_u) + Sb(^4S_u)$, $Ga(^2P_u) + Sb(^2D_u)$, and $Ga(^2P_u) + Sb(^2P_u)$ are computed. However, curves of 11 Λ−S states which dissociate into higher limits are also investigated. Spectroscopic properties of 22 Λ−S states are estimated. The ground state ($X^3\Sigma^-$) of GaSb is described by the $...\sigma^2\pi^2$ configuration with $r_e = 2.82$ Å and $\omega_e = 161$ cm^{-1}. The ground-state dissociation energy (D_e) of GaSb has been calculated to be 1.30 eV. All 22 Λ−S states correlating with the lowest two asymptotes are allowed to mix through the spin−orbit coupling. The spin−orbit effects on the spectroscopic properties of low-lying states up to 22 000 cm^{-1} are investigated. Several dipole-allowed transitions are predicted. The radiative lifetimes of four excited triplet and two singlet states of GaSb are also estimated. Transitions such as $A^3\Pi - X^3\Sigma^-$ and $4^1\Sigma^+ - 2^1\Sigma^+$ are highly probable. The $A^3\Pi$ and $4^1\Sigma^+$ states are found to be short-lived.

I. Introduction

Over the past 2 decades,[1−37] theoretical and experimental studies of the compounds of groups III and V have been carried out in large number mainly because of the technological importance of these materials. Compounds such as GaP, InP, GaAs, InSb, GaSb, InAs, etc., and their neutral and ionic clusters of various sizes are good semiconductors which are used in the preparation of electronic devices. In this regard the pioneering work of Smalley and co-workers[1−6] on clusters of gallium arsenide should be mentioned. Many other successive studies on the electronic structure and spectroscopic features have been carried out by the same group of workers by using the laser photoionization followed by the time-of-flight mass spectrometry measurements. Recently, Lemire et al.[7] have investigated the spectroscopy and electronic structure of the jet-cooled GaAs molecule by the resonant two-photon ionization spectroscopy. The negative ion zero-electron kinetic photodetachment spectroscopic techniques to probe the electronic states of the neutral group IV and group III−V clusters have been employed by Neumark and co-workers.[8−11] The neutral and ionic clusters of indium phosphides have also been studied by these authors. The matrix-isolated electron spin resonance (ESR) spectra of small clusters such as Ge_2, Si_2, Sn_2, and Ga_xAs_y, etc., have been investigated by Weltner and co-workers.[13,14] The infrared absorption spectra of diatomic InX (X = P, As, Sb) molecules have been observed by Li et al.[15] after laser vaporizing the corresponding crystals in rare gases and condensing on the gold surface at 4 K. The zero-field splittings of the ground states of these molecules are also estimated. Similar studies have been carried out by these authors for GaX, Ga_2X, and GaX_2 (X = P, As, Sb) molecules.[16] In recent years,[17,18] organogallium−antimony compounds have been synthesized and characterized. Maeda and Watanabe[19] have studied Sb desorption from Sb/GaAs(001) and GaSb(001) by core-level photoelectron spectroscopy. Not many attempts have been made so far to study the electronic structure and spectroscopic aspects of the GaSb molecule.

An extensive review on relativistic effects for heavy molecules and clusters has been made by Balasubramanian.[20,21] Large-scale configuration interaction (CI) calculations such as complete active space self-consistent field (CASSCF)/CI and MRDCI have been carried out on several group III−V semiconductor molecules and their ions. Balasubramanian and co-workers[21−25] have performed CASSCF followed by first-/second-order CI calculations on GaAs and InSb molecules and their ions. Geometries and potential energy curves of trimers such as $InSb_2$, $SbIn_2$, $GaAs_2$, and $AsGa_2$ have been studied by Das and Balasubramanian[26] using CI calculations. Several low-lying electronic states of mixed isomers of gallium and indium phosphides, namely, Ga_2P, GaP_2, Ga_3P_2, Ga_2P_3, In_2P, InP_2, In_2P_3, In_3P_2, and some of their ions, have been investigated by Feng and Balasubramanian.[27−30] Ab initio based MRDCI calculations on the electronic spectrum diatomic molecules such as GaP, InP, GaAs, and InSb have been carried out by Das and co-workers.[31−34] Russo and co-workers[35,36] have used local spin density methods to study the electronic states of clusters such as Sb_2 and Sb_4, etc., and diatomic molecules such as CuIn, AgIn, CuGa, and AgGa, etc. Toscano and Russo[37] have performed similar calculations on AsP and SbP. However, no extensive theoretical or experimental studies on the electronic structure and spectroscopic properties of GaSb have been attempted so far.

In this paper, we report the computational results on the potential energy curves and spectroscopic features of the low-lying electronic states of GaSb by using MRDCI methods which include relativistic effects. Effects of the spin−orbit coupling on the electronic states up to 22 000 cm^{-1} of energy have been

* To whom correspondence should be addressed. Fax: 91-33-4731484. E-mail: kalyankd@hotmail.com.

10.1021/jp002004w CCC: $19.00
Published on Web 10/07/2000

investigated. Transition probabilities of dipole-allowed transitions and radiative lifetimes of some excited states are also estimated from CI energies and wave functions.

II. Method of Computations

Both gallium and antimony are relatively heavy atoms consisting of many electrons. It is, therefore, essential to employ pseudopotentials of these atoms to reduce the number of active electrons in the calculation. RECP of Ga and Sb are taken from Hurley et al.[38] and LaJohn et al.,[39] respectively. These are semicore types of relativistic effective core potentials (RECP) in which $3d^{10}4s^24p$ electrons of Ga and $4d^{10}5s^25p^3$ electrons of Sb are placed in the valence space while the remaining inner electrons are replaced by effective potentials. Therefore, the number of active electrons in the calculation is reduced to 28. The primitive Gaussian basis functions (3s3p4d) for Ga are taken from Hurley et al.,[38] while, for Sb, the (3s3p4d) functions of La John et al.[39] are augmented with additional s and p functions. The exponents of these augmented s and p functions of Sb are 0.0284 and 0.0276, respectively, which are taken from Balasubramanian.[25] Thus, the final basis set for Sb becomes (4s4p4d), which is sufficient to polarize 5p orbitals of the atom. Both these basis sets are compatible with the RECP used in the calculation. A set of self-consistent-field (SCF) calculations have been performed at each internuclear separation for the $^3\Sigma^-$ state of GaSb with 28 valence electrons. The optimized symmetry-adapted SCF-MOs are used as basis functions for the CI calculations. To reduce the number of configurations, 20 inner electrons, which are mainly occupying 3d and 4d shells of Ga and Sb, respectively, are kept frozen in CI steps. These electrons do not participate in the formation of the Ga−Sb bond in the low-lying electronic states of the molecule. Therefore, only eight active electrons are used in the generation of configurations.

The MRDCI codes of Buenker and co-workers[40−45] have been employed in the present calculations. The Λ−S states are calculated first without any spin−orbit coupling but with all other spin-independent relativistic effects through RECP. The molecule is placed along the *z*-axis. The computations have been carried out in the C_{2v} subgroup of the actual $C_{\infty v}$ group of the molecule. In each irreducible representation of C_{2v}, the lowest eight roots are optimized for singlet, triplet, and quintet spin multiplicities separately. For each Λ−S symmetry in a given spin multiplicity, a set of important reference configurations is selected. These reference configurations define the low-lying excited states of the molecule. All possible single and double excitations are allowed from each reference configuration in the set. This will generate a large number of configurations in the CI space. The generated CI space is of the order of a million in size. A configuration selection[40,41] has been made with a threshold of 1 μhartree. With this choice of configuration-selection threshold, the sums of the squares of coefficients of the reference configurations for the lowest few roots remain in the range 0.91−0.95. Therefore, the configuration-selection procedure reduces the size of the CI space drastically without loosing much accuracy. The energy-extrapolation technique and Davidson's correction[46,47] provide an accurate estimate of the full-CI energy. Potential energy curves of all low-lying Λ−S states are obtained from these CI energies. The bound curves are fitted into polynomials to estimate spectroscopic constants.

The spin−orbit operators of Ga and Sb atoms are obtained from Hurley et al.[38] and LaJohn et al.,[39] respectively. The computations have been performed in A_1, A_2, and B_1 representations of the $C_{2v}{}^2$ group. The Λ−S CI energies are placed in the diagonals, while the off-diagonal Hamiltonian matrix elements are computed from spin−orbit operators and Λ−S CI wave functions. The spin included full-CI-estimated energies are obtained from the eigenvalues of this super-CI calculations. In the present spin−orbit treatment, all Ω components of 22 Λ−S states which correlate with the lowest two limits, namely, $^2P_u(Ga) + {}^4S_u(Sb)$ and $^2P_u(Ga) + {}^2D_u(Sb)$ are included for interactions.

TABLE 1: Dissociation Correlation between the Molecular and Atomic States of GaSb in the Absence of the Spin−Orbit Interaction

Λ−S states	atomic states	rel energy/cm^{-1} expt[a]	rel energy/cm^{-1} calc
$^3\Sigma^-$, $^3\Pi$, $^5\Sigma^-$, $^5\Pi$	$^2P_u(Ga) + {}^4S_u(Sb)$	0	0
$^1\Sigma^+$, $^1\Sigma^-(2)$, $^1\Pi(3)$, $^1\Delta(2)$, $^1\Phi$, $^3\Sigma^+$, $^3\Sigma^-(2)$, $^3\Pi(3)$, $^3\Delta(2)$, $^3\Phi$	$^2P_u(Ga) + {}^2D_u(Sb)$	9 352	12 353
$^1\Sigma^+(2)$, $^1\Sigma^-$, $^1\Pi(2)$, $^1\Delta$, $^3\Sigma^+(2)$, $^3\Sigma^-$, $^3\Pi(2)$, $^3\Delta$	$^2P_u(Ga) + {}^2P_u(Sb)$	17 948	18 530

[a] Moore's table 49; energies are averaged over *j*.

The nuclear Schrödinger equations are solved numerically[48] by using potentials to which the potential energy curves of the Λ−S and Ω states are fitted. The electric dipole transition moments are computed for the pair of vibrational functions of a particular transition. Einstein coefficients of spontaneous emission and transition probabilities are calculated. Radiative lifetimes of the excited states at different vibrational levels are estimated from the transition probability data.

III. Discussion of the Results

Potential Energy Curves of Low-Lying Λ-S States and Their Spectroscopic Properties. In Table 1, we have shown the dissociation relationship between the atomic and molecular states of GaSb in the absence of any spin−orbit mixing. The lowest limit $^2P_u(Ga) + {}^4S_u(Sb)$ correlates with four Λ−S states of triplet and quintet spin multiplicities. On the other hand, the ground state (^2P_u) of Ga combines with the first excited state (^2D_u) of the Sb atom to generate 18 Λ−S states of singlet and triplet multiplicities. The calculated relative energy of the $^2P_u(Ga) + {}^2D_u(Sb)$ limit is found to be higher than the experimental value by about 3000 cm^{-1}. The earlier MRDCI calculations at the similar level on isoelectronic molecules such as GaP, GaAs, InP, and InSb have shown such discrepancies of similar magnitude. The experimental values are, however, averaged over *j* for comparison. The energy of the next higher dissociation limit $^2P_u(Ga) + {}^2P_u(Sb)$, which corresponds to the 12 Λ−S states as shown in Table 1, is in better agreement with the observed data. We have computed all 34 Λ−S states which converge with the three lowest dissociation limits of the molecule. Besides, several high-lying states mostly of triplet and quintet multiplicities are also calculated. All triplet and quintet potential energy curves of GaSb are shown in Figure 1a, while the singlet-state curves are plotted in Figure 1b. Spectroscopic constants (r_e, T_e, and ω_e) of bound Λ−S states as obtained from the MRDCI calculations are summerized in Table 2. As expected, the ground state of GaSb is $X^3\Sigma^-$ with $r_e = 2.82$ Å and $\omega_e = 161$ cm^{-1}. It is mainly described by an open shell configuration $...\sigma_3{}^2\pi^2$ ($c^2 = 0.90$). Not much experimental or theoretical data for the GaSb molecule are available in the literature. However, the far-infrared spectra[16] of the $^{69}Ga^{121}Sb$ molecule in rare gas matrices at 4 K show that the vibrational frequency is about 173 cm^{-1}, which agrees very well with the calculated value of the ground-state GaSb molecule.

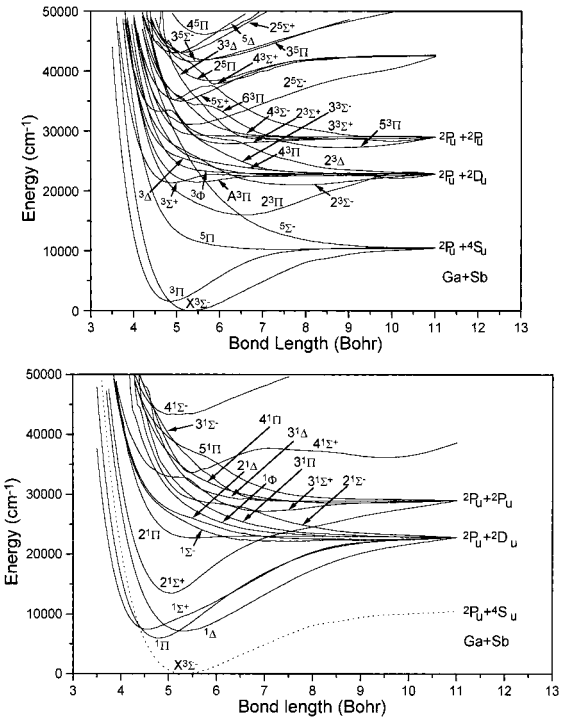

Figure 1. Potential energy curves of (a, top) triplet and quintet and (b, bottom) singlet Λ−S states of GaSb.

TABLE 2: Spectroscopic Constants of Low-Lying Λ−S States of GaSb

state	T_e/cm^{-1}	r_e/Å	ω_e/cm^{-1}
$X^3\Sigma^-$	0	2.82	161 (173)[a]
$^3\Pi$	1 573	2.57	203
$^1\Pi$	5 967	2.54	227
$^1\Delta$	7 150	2.81	171
$^1\Sigma^+$	7 450	2.41	230
$2^1\Sigma^+$	13 582	2.66	241
$2^3\Pi$	16 009	3.47	97
$^3\Sigma^+$	21 383	2.58	175
$A^3\Pi$	21 508	2.90	113
$3^1\Sigma^+$	27 218	3.70	83
$2^3\Sigma^+$	27 914	3.28	77
$2^5\Sigma^-$	31 120	2.81	147
$4^1\Sigma^+$	32 975	2.80	143
$^5\Sigma^+$	35 034	2.69	176
$2^5\Pi$	38 425	3.05	128
$3^5\Pi$	41 622	2.86	140
$3^5\Sigma^-$	41 979	3.01	111
$^5\Delta$	43 070	2.62	196
$2^5\Sigma^+$	43 159	2.73	181
$4^1\Sigma^-$	43 191	2.72	174
$4^5\Pi$	46 190	2.98	154

[a] Experimental value.[16]

The strongly bound singlet states such as $^1\Delta$ and $2^1\Sigma^+$ have the same dominating configurations as those of the ground state (see Table 3). However, the $2^1\Sigma^+$ state is less pure at r_e, where the contributions of $...\pi^4$ ($c^2 = 0.12$) and $...\pi^3\pi$ ($c^2 = 0.1$) configurations are significant. On the otherhand, the r_e and ω_e values of $^1\Delta$ are comparable with those of the ground state. It is lying 7150 cm^{-1} above the ground state, while for the $2^1\Sigma^+$ state the transition energy is 13 582 cm^{-1}. The Ga−Sb bond in the $2^1\Sigma^+$ state is comparatively strong with $r_e = 2.66$ Å and $\omega_e = 241$ cm^{-1}. There is a strong avoided crossing between the curves of $2^1\Sigma^+$ and $^1\Sigma^+$ states at around 5.2 a_o. Although such an avoided crossing is not very prominent in the potential energy curve, there is a slight change in the curvature of the $^1\Sigma^+$ curve near $r = 5.3$ a_o (see Figure 1b). The compositions of CI wave functions of these two low-lying $^1\Sigma^+$ states confirm that two dominant configurations, $...\pi^4$ and $...\sigma_3^2\pi^2$ interchange at the longer bond length region. However, spectroscopic constants of these states are estimated by fitting the adiabatic curves. The Ga−Sb bond in the $^1\Sigma^+$ state is the shortest ($r_e = 2.41$ Å) among all low-lying states studied here. It has a comparatively large vibrational frequency ($\omega_e = 230$ cm^{-1}) with a sharp potential well. At r_e, the $^1\Sigma^+$ state is mainly composed of a closed shell $...\pi^4$ ($c^2 = 0.52$) and an open shell $...\pi^3\pi$ ($c^2 = 0.25$) configurations. The $^1\Sigma^+$ state is lying very close to $^1\Delta$, while other spectroscopic parameters of these two states vary widely. It may be noted that $X^3\Sigma^-$, $^1\Delta$, and $2^1\Sigma^+$ states originating from the same configuration, dissociate into three different asymptotes in the increasing order of energy, while the curve of $^1\Sigma^+$ converges with the ^2P_u(Ga) + ^2D_u(Sb) limit as shown in Figure 1b.

Table 3 shows that a $\sigma_3 \rightarrow \pi$ single excitation gives rise to the first excited state of the $^3\Pi$ symmetry. However, another configuration ($...\sigma_3\pi^2\pi$) contributes significantly in the description of the $^3\Pi$ state, which is only 1573 cm^{-1} above the ground state. The bond length in the $^3\Pi$ state is much shorter compared to that of the ground state. The potential well of the $^3\Pi$ state is quite deep. The same configuration $...\sigma_3\pi^3$ also generates the $^1\Pi$ state, which is 4394 cm^{-1} above the $^3\Pi$ state. The $^1\Pi$ state has a shorter bond length and larger ω_e than its triplet counterpart. As seen from Table 3, the compositions of both $^3\Pi$ and $^1\Pi$ states are almost equal. The potential energy curve of $^3\Pi$ correlates with the lowest dissociation limit, while the $^1\Pi$ state dissociates into ^2P_u(Ga) + ^2D_u(Sb). The larger stability of the bond in the $^{1,3}\Pi$ states as compared to the ground state is found to be a general feature for these types of group III−V diatomic molecules.

Figure 1a shows a broad and shallow potential well for the $2^3\Pi$ state of GaSb. Analyzing the composition of the second root of the $^3B_1$ irreducible representation at different bond lengths, it is revealed that there is a strong avoided crossing between $^3\Pi$ and $2^3\Pi$ curves. At longer bond lengths the $2^3\Pi$ state is dominated by $...\sigma_3\pi^3$, while in the shorter bond length region the state is mainly described by the $...\sigma_3\pi^2\pi$ configuration. Such an avoided crossing produces the broad minimum around 3.47 Å in the potential energy curve of the $2^3\Pi$ state. We have fitted the adiabatic curve to estimate the spectroscopic constants of $2^3\Pi$. The potential minimum of this state lies 16 000 cm^{-1} above the ground state with $\omega_e = 97$ cm^{-1}. The $...\sigma_3\pi^2\pi$ configuration is known to generate as many as 10 Λ−S states. Of these, $^{1,3}\Phi$ states are repulsive and dissociate into the second limit ^2P_u(Ga) + ^2D_u(Sb), while the repulsive $^5\Pi$ curve correlates with the ground dissociation limit. The remaining seven states are of $^{1,3}\Pi$ symmetries. The lowest two $^3\Pi$ states, namely, $2^3\Pi$ and $3^3\Pi$ are bound, while $4^3\Pi$ and $5^3\Pi$ states are repulsive in nature (see Figure 1a). The $3^3\Pi$ state is designated as $A^3\Pi$ in keeping with the analogous A state of GaAs for which the $A^3\Pi - X^3\Sigma^-$ transition is known experimentally. The $A^3\Pi$ state of GaSb is found to be weakly bound with $r_e = 2.90$ Å and $\omega_e = 113$ cm^{-1}. Although no experimental data are available, one should observe the $A^3\Pi - X^3\Sigma^-$ band for GaSb in the region of 21 500 cm^{-1}. The CI wave function of the $A^3\Pi$ state at r_e shows that the contribution of the $...\sigma_3\pi^2\pi$ configuration is about 82%, while another configuration $...\sigma_2\sigma_3^2\pi^2\pi$ contributes about 5% in the mixture. Figure 1b shows that curves of $2^1\Pi$, $3^1\Pi$, and $4^1\Pi$ states which are characterized by the dominant $...\sigma_3\pi^2\pi$ configuration, are repulsive. The highly excited $5^1\Pi$ and $6^3\Pi$ states computed here are also repulsive and dissociate into the third asymptote.

TABLE 3: Dominant Configurations of Λ−S States near the Equilibrium Bond Length

state	configuration (% contributions)
$X^3\Sigma^-$	$\sigma_1^2\sigma_2^2\sigma_3^2\pi^2$ (90)
$^3\Pi$	$\sigma_1^2\sigma_2^2\sigma_3\pi^3$ (75), $\sigma_1^2\sigma_2^2\sigma_3\pi^2\pi$ (13)
$^1\Pi$	$\sigma_1^2\sigma_2^2\sigma_3\pi^3$ (74), $\sigma_1^2\sigma_2^2\sigma_3\pi^2\pi$ (13), $\sigma_1^2\sigma_2\sigma_3^2\pi^2\pi$ (2)
$^1\Delta$	$\sigma_1^2\sigma_2^2\sigma_3^2\pi^2$ (88)
$^1\Sigma^+$	$\sigma_1^2\sigma_2^2\pi^4$ (52), $\sigma_1^2\sigma_2^2\pi^3\pi$ (25), $\sigma_1^2\sigma_2^2\sigma_3^2\pi^2$ (5), $\sigma_1^2\sigma_2\sigma_3\pi^4$ (4)
$2^1\Sigma^+$	$\sigma_1^2\sigma_2^2\sigma_3^2\pi^2$ (62), $\sigma_1^2\sigma_2^2\pi^4$ (12), $\sigma_1^2\sigma_2^2\pi^3\pi$ (10) $\sigma_1^2\sigma_2^2\sigma_3^2\pi\pi$ (2)
$2^3\Pi$	$\sigma_1^2\sigma_2^2\sigma_3\pi^2\pi$ (43), $\sigma_1^2\sigma_2^2\sigma_3\pi^3$ (38), $\sigma_1^2\sigma_2^2\sigma_4\pi^2\pi$ (4), $\sigma_1^2\sigma_2^2\sigma_4\pi^3$ (2)
$^3\Sigma^+$	$\sigma_1^2\sigma_2^2\pi^3\pi$ (70), $\sigma_1^2\sigma_2^2\pi^2\pi^2$ (7), $\sigma_1^2\sigma_2\sigma_3\pi^3\pi$ (5), $\sigma_1^2\sigma_2\sigma_3\pi^4$ (4), $\sigma_1^2\sigma_2\sigma_3\pi^2\pi^2$ (2)
$A^3\Pi$	$\sigma_1^2\sigma_2^2\sigma_3\pi^2\pi$ (82), $\sigma_1^2\sigma_2\sigma_3^2\pi^2\pi$ (5), $\sigma_1^2\sigma_2\sigma_3^2\pi^3$ (1)
$3^1\Sigma^+$	$\sigma_1^2\sigma_2^2\sigma_3^2\pi\pi$ (56), $\sigma_1^2\sigma_2^2\sigma_3\sigma_4\pi\pi$ (12), $\sigma_1^2\sigma_2^2\pi^2\pi^2$ (8), $\sigma_1^2\sigma_2^2\sigma_3^2\pi^2$ (5), $\sigma_1^2\sigma_2^2\pi^3\pi$ (3)
$2^3\Sigma^+$	$\sigma_1^2\sigma_2^2\sigma_3^2\pi\pi$ (47), $\sigma_1^2\sigma_2^2\pi^3\pi$ (31), $\sigma_1^2\sigma_2^2\pi^2\pi^2$ (6), $\sigma_1^2\sigma_2\sigma_3\pi^2\pi^2$ (1)
$2^5\Sigma^-$	$\sigma_1^2\sigma_2^2\sigma_3\sigma_5\pi^2$ (77), $\sigma_1^2\sigma_2^2\sigma_3\sigma_4\pi^2$ (10)
$4^1\Sigma^+$	$\sigma_1^2\sigma_2^2\pi^4$ (38), $\sigma_1^2\sigma_2^2\pi^3\pi$ (13), $\sigma_1^2\sigma_2\sigma_3\pi^4$ (10), $\sigma_1^2\sigma_2^2\sigma_3^2\pi\pi$ (8), $\sigma_1^2\sigma_2\sigma_3\pi^3\pi$ (6)
$^5\Sigma^+$	$\sigma_1^2\sigma_2\sigma_3\pi^3\pi$ (36), $\sigma_1^2\sigma_2^2\pi^2\pi^2$ (34), $\sigma_1^2\sigma_2\sigma_3\pi^2\pi^2$ (18), $\sigma_1^2\sigma_3^2\pi^2\pi^2$ (1)
$2^5\Sigma^+$	$\sigma_1^2\sigma_2^2\pi^2\pi^2$ (41), $\sigma_1^2\sigma_2\sigma_3\pi^3\pi$ (38), $\sigma_1^2\sigma_2\sigma_3\pi^2\pi^2$ (9)
$3^5\Sigma^-$	$\sigma_1^2\sigma_2^2\sigma_3\sigma_6\pi^2$ (63), $\sigma_1^2\sigma_2^2\sigma_3\sigma_4\pi^2$ (20), $\sigma_1^2\sigma_2^2\sigma_3\sigma_5\pi^2$ (2)
$2^5\Pi$	$\sigma_1^2\sigma_2\sigma_3^2\pi^2\pi$ (64), $\sigma_1^2\sigma_2^2\sigma_4\pi^2\pi$ (10), $\sigma_1^2\sigma_2^2\sigma_3\pi^2\pi$ (5), $\sigma_1^2\sigma_2^2\sigma_6\pi^2\pi$ (4), $\sigma_1^2\sigma_2\sigma_3\sigma_4\pi^2\pi$ (3), $\sigma_1^2\sigma_2\sigma_3\sigma_6\pi^2\pi$ (1)
$3^5\Pi$	$\sigma_1^2\sigma_2^2\sigma_3\pi^2\pi$ (83), $\sigma_1^2\sigma_2\sigma_3^2\pi^2\pi$ (2)
$3^5\Sigma^-$	$\sigma_1^2\sigma_2^2\sigma_3\sigma_6\pi^2$ (63), $\sigma_1^2\sigma_2^2\sigma_3\sigma_4\pi^2$ (20), $\sigma_1^2\sigma_2^2\sigma_3\sigma_5\pi^2$ (2)
$^5\Delta$	$\sigma_1^2\sigma_2\sigma_3\pi^3\pi$ (85), $\sigma_1^2\sigma_2\sigma_3\pi^2\pi^2$ (5)
$2^5\Sigma^+$	$\sigma_1^2\sigma_2^2\pi^2\pi^2$ (41), $\sigma_1^2\sigma_2\sigma_3\pi^3\pi$ (38), $\sigma_1^2\sigma_2\sigma_3\pi^2\pi^2$ (9)
$4^1\Sigma^-$	$\sigma_1^2\sigma_2^2\sigma_3\sigma_4\pi^2$ (79), $\sigma_1^2\sigma_2^2\sigma_3\sigma_5\pi^2$ (8)
$4^5\Pi$	$\sigma_1^2\sigma_2^2\sigma_3\pi^2\pi$ (48), $\sigma_1^2\sigma_2\sigma_3^2\pi^2\pi$ (26), $\sigma_1^2\sigma_2^2\sigma_4\pi^2\pi$ (6), $\sigma_1^2\sigma_2^2\sigma_6\pi^2\pi$ (4), $\sigma_1^2\sigma_2\pi^3\pi^2$ (1), $\sigma_1^2\sigma_2\sigma_3\sigma_4\pi^2\pi$ (1)

The next prominent Λ−S state of GaSb is $^3\Sigma^+$ with a T_e value of 21 383 cm^{-1}. The MRDCI calculations show that the $^3\Sigma^+$ state is reasonably strongly bound with a comparatively shorter bond length (r_e = 2.58 Å). The $^3\Sigma^+$ state is characterized mainly by the $...\pi^3\pi$ (c^2 = 0.7) configuration which is obtained from the closed shell configuration of the $^1\Sigma^+$ state through a single excitation $...\pi^4 \rightarrow ...\pi^3\pi$. Table 3 shows that several other open-shell configurations participate with smaller contributions. Potential energy curves of three more states, viz., $2^3\Sigma^+$, $3^3\Sigma^+$, and $4^3\Sigma^+$ states show a couple of strong avoided crossings around the bond lengths of 5.0 a_o and 6.0 a_o. As a result, a shallow minimum is noted at the longer bond length region (r_e = 3.28 Å, ω_e = 77 cm^{-1}) of the $2^3\Sigma^+$ curve. Such a weakly bound long-distant minimum is situated in the energy region of 27 914 cm^{-1}. A short-distant second minimum also appears around 4.6 a_o in the adiabatic curve of $2^3\Sigma^+$. Because of its strong interaction with the higher $^3\Sigma^+$ curve around 5.0 a_o, this potential well could not be fitted. However, the curve shows that this short-distant minimum is around 33 250 cm^{-1} with respect to the ground state. The MRDCI wave functions show that the $2^3\Sigma^+$ state at r_e is a mixture of two equally dominating configurations such as $...\sigma_3^2\pi\pi$ (c^2 = 0.47) and $...\pi^3\pi$ (c^2 = 0.31). The curve crossings are confirmed from the compositions of CI wave functions at different bond lengths.

Among other singlets, potential energy curves of $3^1\Sigma^+$ and $4^1\Sigma^+$ are significant. A sharp avoided crossing between these two curves is noted at 5.5 a_o. Since the interaction is not quite strong, we have fitted diabatic curves of these two states. The $3^1\Sigma^+$ state has a longer equilibrium bond length (r_e = 3.7 Å) with a shallow minimum (ω_e = 83 cm^{-1}). The CI-estimated T_e value of the $3^1\Sigma^+$ state is about 27 218 cm^{-1}, while that of $4^1\Sigma^+$ is 32 975 cm^{-1}. The diabatic $4^1\Sigma^+$ curve correlates with a higher asymptote. The composition of the $4^1\Sigma^+$ state at r_e shows a complex character, and several configurations contribute strongly. In the dissociation limit, the inclusion some Rydberg functions in the basis set is desired for better accuracy. The lowest three states of the $^1\Sigma^-$ symmetry are repulsive (see Figure 1b), while the next one of the same symmetry is found to have a potential minimum above 40 000 cm^{-1} around 2.72 Å with ω_e = 174 cm^{-1}. The composition of $4^1\Sigma^-$ shows that the $...\sigma_3\sigma_4\pi^2$ configuration dominates. The excited $2^1\Delta$ and $3^1\Delta$ states are repulsive in nature.

The low-lying quintet states such as $^5\Sigma^-$ and $^5\Pi$ are repulsive and dissociate into the ground limit. Several high-lying quintet states of GaSb are also calculated in the present study. Figure 1a shows that $2^5\Sigma^-$, $3^5\Sigma^-$, $2^5\Pi$, $3^5\Pi$, $4^5\Pi$, $^5\Sigma^+$, $2^5\Sigma^+$, and $^5\Delta$ states are all strongly bound and dissociate into higher asymptotes. Most of these states are above 40 000 cm^{-1} of energy. As mentioned earlier, the $^5\Pi$ state originates from the $...\sigma_3\pi^2\pi$ configuration. The repulsive $^5\Sigma^-$ state, which is characterized by the $...\sigma_3\sigma_4\pi^2$ configuration, plays an important role because of its crossings with many other low-lying curves. Once the spin−orbit interaction is taken into consideration, the characteristics of several curves change. The spectroscopic parameters (r_e = 2.81 Å and ω_e = 147 cm^{-1}) of the strongly bound $2^5\Sigma^-$ state are comparable with those of the ground state. The MRDCI-estimated T_e value of this state is 31 120 cm^{-1}. As seen in Figure 1a, there is an avoided crossing of $2^5\Sigma^-$ with the repulsive curve of $^5\Sigma^-$. The $2^5\Sigma^-$ state at the minimum is dominated by an excited configuration such as $...\sigma_3\sigma_5\pi^2$. The $3^5\Sigma^-$ state, which is lying 41 979 cm^{-1} above the ground state, has a longer bond length (r_e = 3.01 Å) and smaller ω_e (=111 cm^{-1}) and is composed of $...\sigma_3\sigma_6\pi^2$ configuration. Both $^5\Sigma^+$ and $2^5\Sigma^+$ states are strongly bound, having similar values of r_e and ω_e. The energy separation between these two states is about 8125 cm^{-1}. Two configurations such as $...\sigma_2\sigma_3\pi^3\pi$ and $...\sigma_2^2\pi^2\pi^2$ contribute almost equally in characterizing both $^5\Sigma^+$ states. Of the remaining high-lying quintets, the $^5\Delta$ state has a shorter bond length (r_e = 2.62 Å) and it is strongly bound with ω_e = 196 cm^{-1}. The MRDCI calculated T_e value of $^5\Delta$ is about 43 070 cm^{-1}. The state is relatively pure with $...\sigma_2\sigma_3\pi^3\pi$ (c^2 = 0.83) as the dominating configuration. The $2^5\Pi$, $3^5\Pi$, and $4^5\Pi$ states are bound and dissociate into higher limits (see Figure 1a). The $2^5\Pi$ state having T_e = 38 425 cm^{-1} is composed of at least two excited configurations such as $...\sigma_2\sigma_3^2\pi^2\pi$ (c^2 = 0.64) and $...\sigma_2^2\sigma_4\pi^2\pi$ (c^2 = 0.1), while $3^5\Pi$ is dominated by $...\sigma_2^2\sigma_3\pi^2\pi$ (c^2 = 0.83). The transition energy of the $4^5\Pi$ state is estimated to be 46 190 cm^{-1}. This state is also a mixture of two important configurations, namely, $...\sigma_2^2\sigma_3\pi^2\pi$ (c^2 = 0.48) and $...\sigma_2\sigma_3^2\pi^2\pi$ (c^2 = 0.26).

It may be noted that some wiggles appear in some of the dissociation curves of higher states of the molecule. These are mainly due to insufficient number of points for fitting the

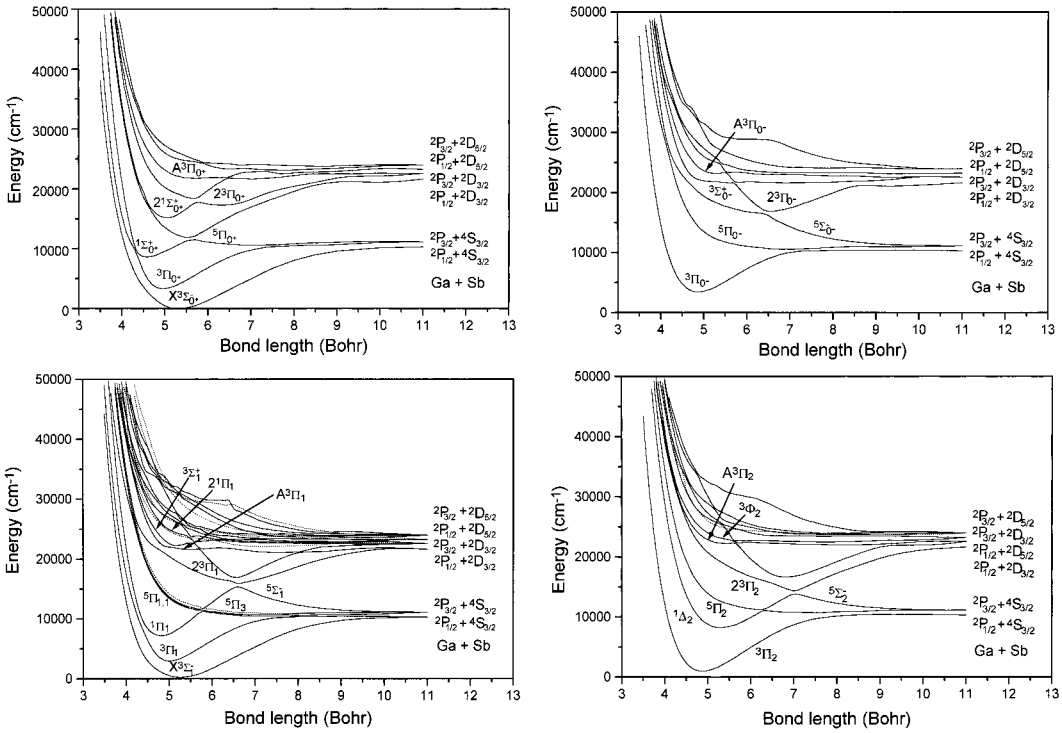

Figure 2. Potential energy curves of the low-lying (a, top, left) 0^+, (b, top, right) 0^-, (c, bottom left) 1 and 3 (curves with dashed line are for $\Omega = 3$), and (d, bottom right) 2 and 4 states of GaSb (the curve with dashed line is for $\Omega = 4$).

potential energy curves near the dissociation limits. However, the trends toward the limits are correct.

The dissociation energy (D_e) of the ground state ($X^3\Sigma^-$) of GaSb is calculated to be 1.3 eV without considering any d-electron correlation and spin−orbit interaction. There are no experimental or other theoretical data available for comparison. Earlier calculations on isoelectronic group III−V molecules suggest that the calculated D_e is always smaller than the observed value by 0.3−0.5 eV. Meier[50] has shown an improvement of D_e by about 0.2 eV due to the d-correlation for GaAs. The MRDCI calculations at the present level have shown that the D_e value of GaP is improved by about 0.14 eV due to the d-correlation and basis set extension. The present calculations have used sufficiently large basis sets and small configuration selection threshold. Therefore, we do not expect significant improvement of D_e by enhancing the basis set and reducing the selection threshold further. An improvement will always be there if $3d^{10}$ electrons of Ga and $4d^{10}$ electrons of Sb are correlated in the CI step. However, some discrepancy is also expected because of the use of effective core potential approximations.

Potential Energy Curves and Spectroscopic Parameters of Low-Lying Ω States. In the calculations of Λ−S states, all relativistic effects except the spin−orbit coupling are included. Once the spin−orbit interaction is introduced through the inclusion of the spin−orbit operators derived from RECPs, all Λ−S states which have the same Ω components will mix. The spin−orbit integrals are evaluated by using spin−orbit operators of Ga and Sb taken from Hurley et al.[38] and LaJohn et al.,[39] respectively. All 22 Λ−S states which correlate with the lowest two dissociation limits are included for the spin−orbit coupling, and these two dissociation limits split into six asymptotes. Relative energies of these asymptotes and their correlations with Ω states are shown in Table 4. The observed spin−orbit splitting ($^2P_{3/2}-{}^2P_{1/2}$) of Ga agrees quite well with the calculated value. The $^2D_{5/2}-{}^2D_{3/2}$ separation of Sb is found to be in the range of 1350−1400 cm^{-1}, while the experimental value is about 1342 cm^{-1}. The disagreement is within the limit of accuracy of the MRDCI calculations which use the effective core potential approximation. However, a large discrepancy of about 3000 cm^{-1} between $^2P_u(Ga) + {}^4S_u(Sb)$ and $^2P_u(Ga) + {}^2D_u(Sb)$ limits (see Table 1) is retained even after the inclusion of the spin−orbit interaction. Therefore, four limits arising from the $^2P_u(Ga) + {}^2D_u(Sb)$ asymptote are higher than the experimental value by about 3000 cm^{-1}. This is probably due to the underestimation of the ground-state dissociation energy. However, this cannot be confirmed because of the nonavailability of any experimental or other theoretical data. All six dissociation limits correlate with Ω states of 0^+, 0^-, 1, 2, 3, and 4 symmetries. Parts a−d of Figure 2 show potential energy curves of all 51 Ω states of which only 15 states are bound and others are repulsive in nature. The fitted spectroscopic constants of these bound states are displayed in Table 5.

TABLE 4: Dissociation Correlation between the Atomic States and Ω States of GaSb

Ω state	atomic state Ga + Sb	rel energy/cm^{-1} expt[a]	rel energy/cm^{-1} calc
2, 1, 1, 0^+, 0^-	$^2P_{1/2} + {}^4S_{3/2}$	0	0
3, 2, 2, 1, 1, 1, 0^+, 0^+, 0^-, 0^-	$^2P_{3/2} + {}^4S_{3/2}$	826	821
2, 1, 1, 0^+, 0^-	$^2P_{1/2} + {}^2D_{3/2}$	8 512	11 450
3, 2, 2, 1, 1, 1, 0^+, 0^+, 0^-, 0^-	$^2P_{3/2} + {}^2D_{3/2}$	9 338	12 258
3, 2, 2, 1, 1, 0^+, 0^-	$^2P_{1/2} + {}^2D_{5/2}$	9 854	12 806
4, 3, 3, 2, 2,2, 1, 1, 1, 1, 0^+, 0^+, 0^-, 0^-	$^2P_{3/2} + {}^2D_{5/2}$	10 680	13 657

[a] Experimental energies are taken from Moore's table.[49]

The zero-field splitting [$^3\Sigma^-(1X_2)-{}^3\Sigma^-(0^+X_1)$] of the ground state of GaSb is about 218 cm^{-1}. The present calculations predict the $X^3\Sigma^-{}_{0^+}$ component to be lower in energy than the other component $X^3\Sigma^-{}_1$. The r_e and ω_e values of these two components are not significantly different. It may be noted that both $X^3\Sigma^-{}_{0^+}$ and $X^3\Sigma^-{}_1$ substates do not remain as pure $X^3\Sigma^-$ because of the nearby 0^+ and 1 components of some other states with which these interact. After the spin−orbit mixing, the lowest substate ($X^3\Sigma^-{}_{0^+}$) has about 5% $^3\Pi$ and 3% $^1\Sigma^+$ contributions

TABLE 5: Spectroscopic Constants of Low-Lying Ω States of GaSb

state	T_e/cm^{-1}	r_e/Å	ω_e/cm^{-1}	dominant Λ−S states near r_e[a]
$X^3\Sigma^-_{0^+}$	0	2.81	149	$X^3\Sigma^-$ (90), $^3\Pi$ (5), $^1\Sigma^+$ (3)
$X^3\Sigma^-_1$	218	2.77	148	$X^3\Sigma^-$ (83), $^3\Pi$ (13), $^1\Pi$ (3)
$^3\Pi_2$	977	2.58	199	$^3\Pi$ (96), $^1\Delta$ (3)
$^3\Pi_1$	3 002	2.65	218	$^3\Pi$ (69), $X^3\Sigma^-$ (29)
$^3\Pi_{0^+}$	3 315	2.62	219	$^3\Pi$ (82), $X^3\Sigma^-$ (11), $2^1\Sigma^+$ (6)
$^3\Pi_{0^-}$	3 443	2.58	200	$^3\Pi$ (98)
$^1\Pi_1$	7 212	2.54	233	$^1\Pi$ (93), $^3\Pi$ (4), $X^3\Sigma^-$ (3)
$^1\Delta_2$	8 251	2.81	179	$^1\Delta$ (94), $^3\Pi$ (5)
$^1\Sigma^+_{0^+}$	8 505	2.42	268	$^1\Sigma^+$ (97)
$2^3\Pi_2$	14 860	3.67	118	$2^3\Pi$ (58), $^5\Sigma^-$ (38)
$2^1\Sigma^+_{0^+}$	15 159	2.67	245	$2^1\Sigma^+$ (92), $^3\Pi$ (4), $X^3\Sigma^-$ (3)
$2^3\Pi_1$	16 160	3.50	120	$2^3\Pi$ (56), $^5\Sigma^-$ (32), $^1\Pi$ (8)
$2^3\Pi_{0^-}$	16 976	3.51	161	$2^3\Pi$ (84), $^5\Sigma^-$ (7), $2^3\Sigma^+$ (2)
$2^3\Pi_{0^+}$	18 500	2.97	217	$2^3\Pi$ (94), $3^1\Delta$ (2)
$A^3\Pi_{0^+}$	21 771	3.03	89	$A^3\Pi$ (94), $5^3\Pi$ (2)

[a] Values in parentheses refer to the percentage contributions.

near r_e, while for the upper component ($X^3\Sigma^-_1$), the contribution of $^3\Pi$ is as large as 13%. Four Ω components of $^3\Pi$ are split as 2, 1, 0^+, and 0^- in the ascending order of energy. The largest splitting is calculated to be 2466 cm^{-1}. The $^3\Pi_2$ and $^3\Pi_{0^-}$ components remain as pure $^3\Pi$ because there are no nearby components of the corresponding symmetries for coupling. The other two components $^3\Pi_{0^+}$ and $^3\Pi_1$ couple strongly with $X^3\Sigma^-_{0^+}$ and $X^3\Sigma^-_1$, respectively. Moreover, there are some strong avoided crossings near the minima of the potential energy curves of 0^+ and 1 components of $^3\Pi$. Spectroscopic constants of these components are estimated by fitting the adiabatic curves. The fitted constants of $^3\Pi_{0^+,1}$ components, therefore, change to a considerable extent. Table 5 shows that 69% $^3\Pi$ and 29% $X^3\Sigma^-$ states contribute toward the formation of $^3\Pi_1$ at r_e, while in $^3\Pi_{0^+}$ some contribution comes from the high-lying state like $2^1\Sigma^+$. The only $^1\Pi_1$ component remains almost unperturbed due to the spin−orbit coupling. However, $^3\Pi_1$ (4%) and $X^3\Sigma^-_1$ (3%) components influence the transition energy of $^1\Pi_1$ to a small extent. The r_e and ω_e values of each component of three successive singlets such as $^1\Delta_2$, $^1\Sigma^+_{0^+}$, and $2^1\Sigma^+_{0^+}$ remain unchanged due to the spin−orbit interaction. However, transition energies of these components are increased by about 1100−1600 cm^{-1}. Figure 2a shows that the potential energy curve of $^1\Sigma^+_{0^+}$ undergoes two sharp avoided crossings: one with the $^3\Pi_{0^+}$ curve around 4.5 a_o and the other with the $^5\Pi_{0^+}$ curve near 5.6 a_o. The $2^1\Sigma^+_{0^+}$ state curve also undergoes avoided crossings with $^5\Pi_{0^+}$ and $2^3\Pi_{0^+}$ before and after the potential minimum. The potential energy curve of the $^1\Delta_2$ component shows two avoided crossings (Figure 2d) at the longer bond length region. The spectroscopic parameters of these components are estimated by fitting the corresponding diabatic curves.

The 2, 1, and 0^- components of the repulsive $^5\Sigma^-$ curve undergo several avoided crossings with other curves of similar Ω components. The curve crossings of these components with those of $2^3\Pi$ and $A^3\Pi$ are significant. As already discussed the appearance of the minimum in the potential energy curve of $2^3\Pi$ is mainly due to the avoided crossing with the low-lying $^3\Pi$ state. After the introduction of the spin−orbit coupling, the potential energy curves become more complicated. The diabatic curves of $2^3\Pi_{0^+}$ and $2^3\Pi_{0^-}$ components would be fitted for estimating the spectroscopic constants. Some of the states in the adiabatic chanels are found to be predissociating. The spin−orbit interaction makes the shallow curves of all four components of $A^3\Pi$ complicated. The $A^3\Pi_{0^-}$, $A^3\Pi_1$, and $A^3\Pi_2$ components interact with the corresponding components of the repulsive $^5\Sigma^-$ state as evident from Figures 2b−d, and hence

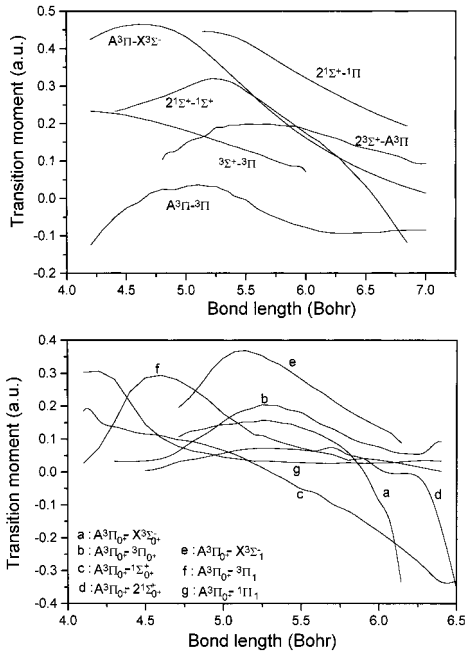

Figure 3. Transition dipole moment functions of (a, top) six transitions among Λ−S states and (b, bottom) 0^+-0^+ and 0^+-1 transitions involving the $A^3\Pi_{0^+}$ component.

TABLE 6: Radiative Lifetimes of Some Excited Λ−S States of GaSb[a]

transition	partial lifetimes (s) of the upper state $v'=0$	$v'=1$	$v'=2$	tot. lifetimes (s) of the upper state at $v'=0$
$2^1\Sigma^+ \rightarrow {}^1\Pi$	7.33(−6)	7.32(−6)	7.32(−6)	
$2^1\Sigma^+ \rightarrow {}^1\Sigma^+$	5.85(−5)	5.88(−5)	5.91(−5)	$\tau(2^1\Sigma^+) = 6.5(-6)$
$^3\Sigma^+ \rightarrow {}^3\Pi$	1.75(−6)	1.80(−6)	1.86(−6)	$\tau(^3\Sigma^+) = 1.3(-6)$
$4^1\Sigma^+ \rightarrow 2^1\Sigma^+$	7.64(−8)	8.12(−8)	8.48(−8)	
$4^1\Sigma^+ \rightarrow {}^1\Sigma^+$	6.34(−7)	1.03(−6)	3.89(−6)	
$4^1\Sigma^+ \rightarrow {}^1\Pi$	4.41(−4)	9.78(−5)	2.45(−5)	$\tau(4^1\Sigma^+) = 1.3(-8)$
$2^3\Pi \rightarrow X^3\Sigma^-$	8.81(−2)	7.23(−3)	1.44(−3)	
$2^3\Pi \rightarrow {}^3\Pi$	9.81(5)	1.09(4)	2.61(2)	$\tau(2^3\Pi) = 8.73(-2)$
$A^3\Pi \rightarrow X^3\Sigma^-$	5.63(−7)	5.91(−7)	6.20(−7)	
$A^3\Pi \rightarrow {}^3\Pi$	2.22(−4)	7.94(−5)	7.28(−5)	$\tau(A^3\Pi) = 5.61(-7)$
$2^3\Sigma^+ \rightarrow A^3\Pi$	8.62(−5)	8.73(−5)	8.29(−5)	
$2^3\Sigma^+ \rightarrow 2^3\Pi$	1.64(−2)	4.82(−3)	2.45(−3)	
$2^3\Sigma^+ \rightarrow {}^3\Pi$	1.58(−1)	1.49(−2)	2.86(−3)	$\tau(2^3\Sigma^+) = 8.57(-5)$

[a] Values in parentheses are powers to base 10.

these substates predissociate. The diabatic curves of these components could not be fitted. Only the $A^3\Pi_{0^+}$ component survives the predissociation, and its spectroscopic constants are given in Table 5. The $A^3\Pi_{0^+}-X^3\Sigma^-_{0^+}$ and $A^3\Pi_{0^+}-X^3\Sigma^-_1$ transitions should take place in the energy region of 27 170 and 21 553 cm^{-1}, respectively.

Radiative Lifetimes of Some Excited Electronic States. Several dipole-allowed transitions are computed from the MRDCI results of GaSb. No experimental or theoretical data are known so far in this regard. We have considered transitions from two singlet states, such as $2^1\Sigma^+$ and $4^1\Sigma^+$, and four triplet states, namely, $^3\Sigma^+$, $2^3\Pi$, $A^3\Pi$, and $2^3\Sigma^+$ to all possible lower states with $\Delta\Lambda = 0, \pm 1$. The calculated transition moments of strong transitions are plotted as a function of the internuclear distance (Figure 3a). Transition probabilities of these dipole-allowed transitions and hence partial lifetimes of the upper states are estimated. In Table 6, we have given partial lifetimes of six excited states at the lowest three vibrational levels involving transitions within 21 000 cm^{-1} of energy. The radiative lifetimes are calculated only at the lowest vibrational level ($v' = 0$).

TABLE 7: Radiative Lifetimes of the $A^3\Pi_{0^+}$ States of GaSb at $v' = 0$

transition	lifetimes (s) of the $A^3\Pi_{0^+}$ state
$A^3\Pi_{0^+} \rightarrow X^3\Sigma^-_{0^+}$	2.93(−5)
$A^3\Pi_{0^+} \rightarrow X^3\Sigma^-_{1}$	2.49(−6)
$A^3\Pi_{0^+} \rightarrow {}^3\Pi_{0^+}$	1.73(−5)
$A^3\Pi_{0^+} \rightarrow {}^3\Pi_{1}$	4.63(−5)
$A^3\Pi_{0^+} \rightarrow {}^1\Sigma^+_{0^+}$	3.11(−4)
$A^3\Pi_{0^+} \rightarrow 2^1\Sigma^+_{0^+}$	2.76(−3)
$A^3\Pi_{0^+} \rightarrow {}^1\Pi_{1}$	1.09(−3)
tot. lifetime (s)	$\tau(A^3\Pi_{0^+}) = 1.93(-6)$

[a] Values in parentheses are powers to base 10.

The transition moment of $2^1\Sigma^+-{}^1\Pi$ at any bond length is found to be always higher than that of the $2^1\Sigma^+-{}^1\Sigma^+$ transition. The Franck−Condon overlap factor of the former transition is also higher. Considering only these two transitions, the radiative lifetime of $2^1\Sigma^+$ is calculated to be 6.5 μs at $v' = 0$. The $^3\Sigma^+-{}^3\Pi$ transition should be reasonably strong, and the computed radiative lifetime of the $^3\Sigma^+$ state is of the order of 1.3 μs. The excited $4^1\Sigma^+$ state may undergo three symmetry-allowed transitions to the lower states such as $^1\Pi$, $^1\Sigma^+$, and $2^1\Sigma^+$. The transition probabilities of $4^1\Sigma^+-2^1\Sigma^+$ and $4^1\Sigma^+-{}^1\Sigma^+$ are large, while the other transition $4^1\Sigma^+-{}^1\Pi$ is much weaker. Summing up transition probabilities of these transitions, the total radiative lifetime of the $4^1\Sigma^+$ state is estimated to be only 13 ns. Two possible transitions involving $2^3\Pi$, namely, $2^3\Pi-X^3\Sigma^-$ and $2^3\Pi-{}^3\Pi$ are very weak. The lifetime of the $2^3\Pi$ state is considerably large, indicating the very low transition probability. As a result of the shallow potential minimum of $2^3\Pi$ arising out of its strong interaction with $^3\Pi$ at the longer bond length region, the Franck−Condon overlap terms are negligibly small.

Transitions involving the $A^3\Pi$ state are significant for these types of group III−V molecules. Figure 3a shows smooth transition-moment curves having maxima for both $A^3\Pi-X^3\Sigma^-$ and $A^3\Pi-{}^3\Pi$ transitions of GaSb. The transition moments of the former transition are much larger than those of the latter. Although the A−X band system for GaSb is not observed yet, the present calculations show that the transition is reasonably strong. The other transition like $A^3\Pi-{}^3\Pi$ is considerably weak. The total radiative lifetime of the $A^3\Pi$ state is estimated to be 561 ns. We have also calculated transition probabilities of transitions from $2^3\Sigma^+$ to three low-lying states of the $^3\Pi$ symmetry. The $2^3\Sigma^+-A^3\Pi$ transition is comparatively strong, while the remaining two transitions such as $2^3\Sigma^+-2^3\Pi$ and $2^3\Sigma^+-{}^3\Pi$ are very weak. The plot of transition moments for $2^3\Sigma^+-A^3\Pi$ as a function of the internuclear distance is shown in Figure 3a. The overall radiative lifetime of the $2^3\Sigma^+$ state is computed to be about 85.7 μs.

After the inclusion of the spin−orbit coupling several changes occur in the potential energy curves. The $A^3\Pi_{0^+}$ component which survives the predissociation undergoes several transitions with $\Delta\Omega = 0, \pm1$. Table 7 shows the list of these transitions involving the $A^3\Pi_{0^+}$ component at $v' = 0$. Four transitions are of the 0^+-0^+ type, while others are of the 0^+-1 type. Of these, $A^3\Pi_{0^+}-X^3\Sigma^-_{0^+}$ and $A^3\Pi_{0^+}-X^3\Sigma^-_{1}$ transitions are found to be stronger than others. Transition moments of all seven transitions are plotted as a function of the bond length in Figure 3b. The present calculations predict that the total radiative lifetime of the $A^3\Pi_{0^+}$ component at $v' = 0$ is about 1.93 μs (Table 7). However, no data are available for comparison.

Comparison with the Isovalent GaP and GaAs. Electronic structure and spectroscopic properties of GaP and GaAs have been thoroughly studied recently by performing MRDCI calculations which involve the spin−orbit coupling.[31,33] The results of GaSb which is the next heavier diatomic molecule of gallium in this group may be compared with those of GaP and GaAs. The ground states of all three gallium molecules are of the $X^3\Sigma^-$ symmetry with the dominant configuration $...\sigma_3^2\pi^2$. The ground-state equilibrium bond lengths of these molecules are in the expected order as r_e(GaP) < r_e(GaAs) < r_e(GaSb). The ω_e values are also in the desired trend. The MRDCI calculations at the same level have shown somewhat smaller ($^1\Pi-{}^3\Pi$) energy splitting for GaSb, while for GaP and GaAs, such splittings are of comparable magnitudes. The energy spectrum and potential energy curves of the low-lying states of three molecules are similar. The transition energy of the $^3\Pi$ state increases from the lighter (GaP) to the heavier (GaSb) molecule. The equilibrium bond lengths of the $^3\Pi$ state of all three molecules are shorter than the ground-state r_e by about 0.25 Å. For these types of group III−V diatomic molecules, the $^3\Pi$ state with $...\sigma_3\pi^3$ as the dominating configuration is generally more stable than $^1\Sigma^+$ which has a closed-shell configuration. The $^1\Sigma^+-{}^3\Pi$ energy separation is found to be the largest for GaSb, indicating the greater stability of the $^3\Pi$ state as compared with $^1\Sigma^+$ for the heavier molecule. The ground-state dissociation energy of GaP is 1.69 eV, while for GaAs and GaSb, the D_e values are about 1.3 eV. The $A^3\Pi-X^3\Sigma^-$ transition of GaAs has been extensively studied by many authors, while for GaP and GaSb it is seldom studied. The MRDCI-estimated transition energies of the A−X transition for GaP, GaAs, and GaSb fall in the region of 21 000−24 000 cm^{-1}. The heavier molecule GaSb has a smaller transition energy as per expectation. A double minimum appears in the potential energy curve of the $2^3\Sigma^+$ state for all three molecules due to its avoided crossing with the curve of $^3\Sigma^+$. The nature of three $^1\Sigma^+$ curves of these molecules is also similar. It may be noted that there exists a strong interaction between the curves of $^1\Sigma^+$ and $2^1\Sigma^+$ states, while a large energy gap does not allow any mixing of $2^1\Sigma^+$ with $3^1\Sigma^+$ for all three molecules of gallium compared here. A sharp avoided crossing is noticed between $3^1\Sigma^+$ and $4^1\Sigma^+$ curves of all three molecules. The diabatic curves of the $4^1\Sigma^+$ state of GaP, GaAs, and GaSb molecules are remarkably similar. However, the existence of the $4^1\Sigma^+$ state for these types of molecules is not yet known.

The long-distant broad potential well of the $2^3\Pi$ state of GaSb looks very similar with that of GaP and GaAs. For all three molecules the minimum appears due to an avoided crossing between the strongly bound $^3\Pi$ curve and a repulsive curve of the excited $2^3\Pi$ state. There are no avoided crossings between $2^3\Pi$ and $A^3\Pi$ curves of these molecules. The repulsive $^5\Sigma^-$ curve crosses the potential energy curves of $2^3\Pi$ and $A^3\Pi$ in a similar manner for these molecules. As a result, the 0^-, 1, and 2 components of $A^3\Pi$ predissociate due to their interactions with the corresponding components of $^5\Sigma^-$. Only for GaAs, the predissociations of $A^3\Pi_{0^-}$, $A^3\Pi_1$, and $A^3\Pi_2$ components are observed experimentally, while for GaP and GaSb such predissociations are not observed although a similar situation is predicted from the MRDCI calculations.

IV. Conclusion

MRDCI calculations based on RECP in which 3d, 4s, and 4p electrons of Ga and 4d, 5s, and 5p electrons of Sb are kept in the valence space show that the ground-state symmetry of GaSb is $X^3\Sigma^-$ same as that of isovalent GaP, GaAs, and other group III−V diatomic molecules. At least 21 bound states of GaSb exist within 46 000 cm^{-1} of energy. The ground-state r_e and ω_e of GaSb are 2.82 Å and 161 cm^{-1}, respectively. The

use of RECP in the CI calculations is known to overestimate r_e and underestimate ω_e. The observed ω_e of the ground-state $^{69}Ga^{121}Sb$ is around 173 cm^{-1}, while no experimental r_e is known so far. Two low-lying quintets, namely, $^5\Pi$ and $^5\Sigma^-$ are repulsive, while the remaining eight high-lying quintet states with energy above 30 000 cm^{-1} are strongly bound. The dissociation energy (D_e) of the ground-state GaSb is estimated to be 1.3 eV. It is expected that the d-electron correlation and RECP approximation would underestimate the dissociation energy. Therefore, the observed D_e of GaSb should be 0.3−0.5 eV larger than the calculated value. The $A^3\Pi$ state of GaSb is lying 21 500 cm^{-1} above the ground state with $r_e = 2.90$ Å and $\omega_e = 113$ cm^{-1}. The spin−orbit coupling has been included for 22 Λ−S states which dissociate into the lowest two limits. The zero-field splitting in the ground state of GaSb is predicted to be 218 cm^{-1}, which is larger than that of both GaP and GaAs. Several avoided crossings occur in the potential energy curves of Ω components. The spin−orbit components with $\Omega = 2$, 1, and 0^- of the $A^3\Pi$ state interact with those of the repulsive $^5\Sigma^-$ state resulting their predissociations. Transitions such as $2^1\Sigma^+-1^1\Pi$, $3^1\Sigma^+-3^1\Pi$, $4^1\Sigma^+-2^1\Sigma^+$, $4^1\Sigma^+-1^1\Sigma^+$, $A^3\Pi-X^3\Sigma^-$, and $A^3\Pi-3^3\Pi$ are found to be strong. The $A^3\Pi_{0^+}$ component, which survives from the predissociation undergoes four reasonably strong transitions to $X^3\Sigma^-_{0^+}$, $X^3\Sigma^-_1$, $^3\Pi_{0^+}$, and $^3\Pi_1$. The $A^3\Pi_{0^+}-X^3\Sigma^-_1$ transition is the strongest one and the radiative lifetime of the $A^3\Pi_{0^+}$ component is 1.93 μs at the lowest vibrational level.

Acknowledgment. We are grateful to Prof. Dr. Robert J. Buenker, Wuppertal, Germany, for his kind permission to use his CI codes for the present calculations. The financial support from CSIR under Grant 01(1427)/96/EMR-II is gratefully acknowledged.

References and Notes

(1) O' Brien, S. C.; Liu, Y.; Zhang, Q.; Heath, J. R.; Tittel, F. K.; Curl, R. F.; Smalley, R. E. *J. Chem. Phys.* **1986**, *84*, 4074.
(2) Liu, Y.; Zhang, Q.; Tittel, F. K.; Curl, R. F.; Smalley, R. E. *J. Chem. Phys.* **1986**, *85*, 7434.
(3) Zhang, Q.; Liu, Y.; Curl, R. F.; Tittel, F. K.; Smalley, R. E. *J. Chem. Phys.* **1988**, *88*, 1670.
(4) Wang, L.; Chibante, L. P. F.; Tittel, F. K.; Curl, R. F.; Smalley, R. E. *Chem. Phys. Lett.* **1990**, *172*, 335.
(5) Jin, C.; Taylor, K.; Conciecao, J.; Smalley, R. E. *Chem. Phys. Lett.* **1990**, *175*, 17.
(6) Lou, L.; Wang, L.; Chibante, L. P. F.; Laaksonen, R. T.; Norlanden, P.; Smalley, R. E. *J. Chem. Phys.* **1991**, *94*, 8015.
(7) Lemire, G. W.; Bishea, G. A.; Heidecke, S. A.; Morse, M. D. *J. Chem. Phys.* **1990**, *92*, 121.
(8) Arnold, C. C.; Neumark, D. M. *Can. J. Phys.* **1994**, *72*, 1322.
(9) Xu, C.; de Beer, E.; Arnold, D. W.; Arnold, C. C.; Neumark, D. M. *J. Chem. Phys.* **1994**, *101*, 5406.
(10) Arnold, C. C.; Neumark, D. M. *J. Chem. Phys.* **1994**, *99*, 3353.
(11) Arnold, C. C.; Neumark, D. M. *J. Chem. Phys.* **1994**, *100*, 1797.
(12) Burton, G. R.; Xu, C.; Arnold, C. C.; Neumark, D. M. *J. Chem. Phys.* **1996**, *104*, 2757.
(13) Van Zee, R. J.; Li, S.; Weltner, W., Jr. *J. Chem. Phys.* **1993**, *98*, 4335.
(14) Li, S.; Van Zee, R. J.; Weltner, W., Jr. *J. Chem. Phys.* **1994**, *100*, 7079.
(15) Li, S.; Van Zee, R. J.; Weltner, W., Jr. *J. Phys. Chem.* **1994**, *98*, 2275.
(16) Li, S.; Van Zee, R. J.; Weltner, W., Jr. *J. Phys. Chem.* **1993**, *97*, 11393.
(17) Foas, E. E.; Jouet, R. J.; Wells, R. L.; Rheingold, A. L.; Liable-Sands, L. M. *J. Organomet. Chem.* **1999**, *582*, 45.
(18) Schulz, S.; Nieger, M. *J. Organomet. Chem.* **1998**, *570*, 275.
(19) Maeda, F.; Watanabe, Y. *J. Electron Spectrosc. Relat. Phenom.* **1999**, *101*, 293.
(20) Balasubramanian, K. *Relativistic Effects in Chemistry Part A. Theory and Techniques*; Wiley-Interscience: New York, 1997.
(21) Balasubramanian, K. *Relativistic Effects in Chemistry Part B. Applications to Molecules and Clusters*; Wiley-Interscience: New York, 1997.
(22) Balasubramanian, K. *Chem. Rev.* **1990**, *90*, 93.
(23) Balasubramanian, K. *J. Chem. Phys.* **1987**, *86*, 3410. Erratum: Balasubramanian, K. *J. Chem. Phys.* **1990**, *92*, 2123.
(24) Balasubramanian, K. *J. Mol. Spectrosc.* **1990**, *139*, 405.
(25) Balasubramanian, K. *J. Chem. Phys.* **1990**, *93*, 507.
(26) Das, K. K.; Balasubramanian, K. *J. Chem. Phys.* **1991**, *94*, 6620.
(27) Feng, P. Y.; Balasubramanian, K. *Chem. Phys. Lett.* **1997**, *265*, 41.
(28) Feng, P. Y.; Balasubramanian, K. *Chem. Phys. Lett.* **1997**, *265*, 547.
(29) Feng, P. Y.; Balasubramanian, K. *Chem. Phys. Lett.* **1998**, *283*, 167.
(30) Feng, P. Y.; Balasubramanian, K. *Chem. Phys. Lett.* **1998**, *284*, 313.
(31) Manna, B.; Das, K. K. *J. Mol. Struct. (THEOCHEM)* **1999**, *467*, 135.
(32) Manna, B.; Dutta, A.; Das, K. K. *J. Phys. Chem.* **2000**, *A104*, 2764.
(33) Manna, B.; Das, K. K. *J. Phys. Chem.* **1998**, *A102*, 9876.
(34) Manna, B.; Dutta, A.; Das, K. K. *J. Mol. Struct. (THEOCHEM*) **2000**, *497*, 123.
(35) Oranges, T.; Musolino, V.; Toscano, M.; Russo, N. *Z. Phys. D* **1990**, *17*, 133.
(36) Musolino, V.; Toscano, M.; Russo, N. *J. Comput. Chem.* **1990**, *11*, 924.
(37) Toscano, M.; Russo, N. *Z. Phys. D* **1992**, *22*, 683.
(38) Hurley, M. M.; Pacios, L. F.; Christiansen, P. A.; Ross, R. B.; Ermler, W. C. *J. Chem. Phys.* **1986**, *84*, 6840.
(39) LaJohn, L. A.; Christiansen, P. A.; Ross, R. B.; Atashroo, T.; Ermler, W. C. *J. Chem. Phys.* **1987**, *87*, 2812.
(40) Buenker, R. J.; Peyerimhoff, S. D. *Theor. Chim. Acta* **1974**, *35*, 33.
(41) Buenker, R. J.; Peyerimhoff, S. D. *Theor. Chim. Acta* **1975**, *39*, 217.
(42) Buenker, R. J. *Int. J. Quantum Chem.* **1986**, *29*, 435.
(43) Buenker, R. J.; Peyerimhoff, S. D.; Butcher, W. *Mol. Phys.* **1978**, *35*, 771.
(44) Buenker, R. J. In *Proceedings of the Workshop on Quantum Chemistry and Molecular Physics*; Burton, P., Ed.; University Wollongong: Wollongong, Australia, 1980. *Studies in Physical and Theoretical Chemistry;* Carbó, R., Ed.; Elsevier: Amsterdam, 1981; Vol 21 (Current Aspects of Quantum Chemistry).
(45) Buenker, R. J.; Phillips, R. A. *J. Mol. Struct. (THEOCHEM)* **1985**, *123*, 291.
(46) Davidson, E. R. In *The World of Quantum Chemistry*; Daudel, R., Pullman, B., Eds.; Reidel: Dordrecht, The Netherlands, 1974.
(47) Hirsch, G.; Bruna, P. J.; Peyerimhoff, S. D.; Buenker, R. J. *Chem. Phys. Lett.* **1977**, *52*, 442.
(48) Colley, J. W. *Math. Comput.* **1961**, *15*, 363.
(49) Moore, C. E. *Atomic Energy Levels*; National Bureau of Standards: Washington, DC, 1971; Vol. 3.
(50) Meier, U.; Peyerimhoff, S. D.; Bruna, P. J.; Grein, F. *J. Mol. Spectrosc.* **1989**, *134*, 259.